Journal of the European Ceramic Society 22 (2002) 253–261

www.elsevier.com/locate/jeurceramsoc

The mechanical properties of AlN/Al composites manufactured by squeeze casting

Ding-Fwu Lii[a,*], Jow-Lay Huang[b], Shao-Ting Chang[b]

[a]*Department of Electrical Engineering, Chinese Naval Academy, Kaohsiung, Taiwan 813, Peoples' Republic of China*
[b]*Department of Material Science and Engineering, National Cheng-Kung University, Tainan, Taiwan 701, Peoples' Republic of China*

Received 16 November 2000; received in revised form 2 March 2001; accepted 24 March 2001

Abstract

Porous aluminum nitride (AlN) preform was formed by sintering in N_2 at 1600°C for 1 h. The molten pure Al was infiltrated into the preform to make AlN/Al composite with different compositions by squeeze casting. The AlN composition in AlN/Al composite increased from 51.2 to 70.0% when the pressing pressures of AlN preforms increased from 10 to 60 MPa, respectively. The hardness of the composite increased from 93 to 145 H_v, the fracture strength increased from 328 to 490 MPa, and the compressive strength increased from 210 to 340 MPa for the corresponding composites. The fracture modes in AlN/Al composites included (1) ductile neck fracture in Al, (2) brittle intergranular fracture between smaller AlN grains, (3) brittle transgranular fracture within larger AlN grains. Three crack growth paths along (1) Al/Al interface, (2) AlN/AlN interface, and (3) AlN/Al interface were observed in the AlN/Al composites. The fracture toughness of the squeeze casting AlN/Al composites was between 14.5 and 15.7 MPa $m^{1/2}$. No obvious trend between the fracture toughness and the composition of the composite has been observed. However, the ductility of the composite decreased with the increase of AlN content.

Keywords: Squeeze casting; Infiltration; Fracture; Toughness; AlN/Al composite

1. Introduction

Aluminum nitride (AlN) is a hard refractory ceramic which has been investigated for use as a high-temperature structural ceramic and for substrate and package applications for electronic components because of its extremely high conductivity, good strength and low thermal expansion coefficient.[1–4] Furthermore, AlN is also considered to be applied as a ceramic tile-faced lightweight armor before.[5] However, like other monolithic ceramics, it is apt to suffer from high production cost, low ductility and low fracture toughness. Therefore, metals (e.g. aluminum, cobalt, niobium) or alloys are added into ceramics for the purpose of improving its toughness.[6–10]

Several formation methods of AlN/Al composites have been reported, including directed growth reaction,[11] pressureless liquid metal infiltration,[6] nitrogen plasma-alloy reaction and spray deposition,[12] and pressure metal infiltration.[13] However, in order to manufacture the superior near-net-shape composite engineering components with neither gas porosity nor shrinkage porosity, the squeeze casting method[14,15] could be an alternative for AlN/Al composites. It uniquely allows both the ceramic and the metal phases to retain as extremely fine grains, due to the absence of sintering the ceramic body at high temperature. However, the problems of heterogeneities and the possible existence of veins in squeeze casting still remain to be resolved.

In this study, porous AlN preform was formed by sintering in N_2 at 1600°C for 1 h and the molten pure Al was infiltrated into the preform to make AlN/Al composite by squeeze casting. Carbon black was mixed with AlN powder to increase its wetting ability with metal. In order to control the microstructure of the composite, the preform processing variables such as pressing pressure and additives will be systematically changed. The density and mechanical properties of the composite will be measured and tested. The effects of the composition on the physical and mechanical properties have also been investigated. In addition, the microstructure and fracture behavior of the composite were examined.

* Corresponding author. Tel.: +886-7-5834700-1305; fax: +886-7-5829681.
E-mail address: dflii@mail.cna.edu.tw (D.-F. Lii).

0955-2219/01/$ - see front matter
PII: S0955-2219(01)00255-2

2. Experimental procedure

2.1. Sample preparation

Aluminum nitride powders of medium grain size higher than 5 μm were extracted from the as-received powders (H.C. Stark, Germany) by sedimentation. AlN powder was mixed with 1 wt.% carbon black in isopropanol with a magnetic stirrer for 5 h, including 5 min ultrasonic agitation at the beginning of every hour. Carbowax 4000 (polyethylene glycol, 10 wt.%) was dissolved in trichloroethylene and added to the powder as a binder for specimen pressing. The preparation was dried for 5 h at 40–50°C. Dried agglomerates were ground with an alumina mortar and pestle, and sieved through a 100 mesh (<150 μm) screen for pulverizing the aggregrates.

2.2. Green forming and squeeze casting

Porous AlN preform was formed by sintering in N_2 at 1600°C for 1 h. Then, the molten pure Al was infiltrated into the preform to make Al/AlN composite with different composition by squeeze casting. Fig. 1 shows the schematic of the squeeze-casting process. Four steps were included: (1) molten Al pouring; (2) AlN preform setting (preheated to 750°C); (3) high-pressure (200 MPa) infiltration for 15 s; and (4) release the pressure and extraction of the ingot.

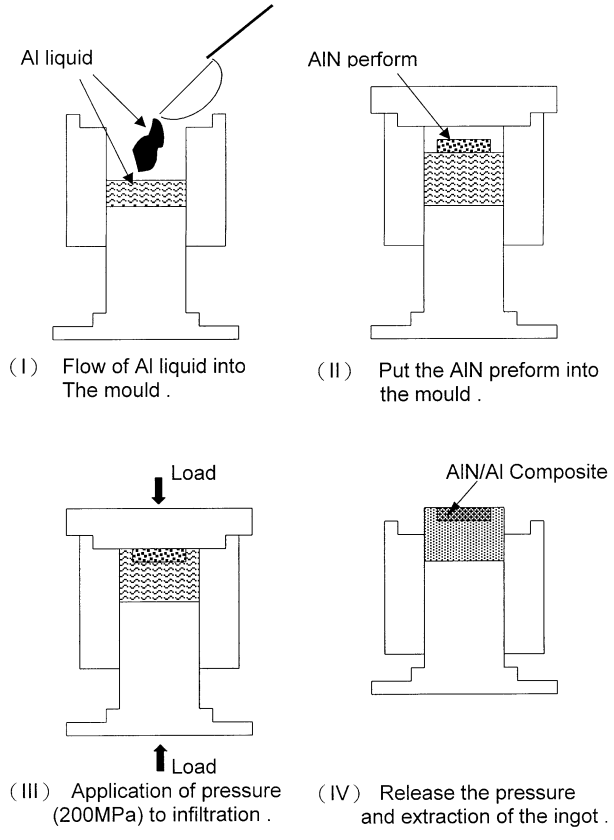

Fig. 1. Schematic of the squeeze-casting process.

2.3. Density and mechanical properties

Density was measured by the water displacement technique. Hardness was determined using Vickers equipment, H_v (Akashi AVK C21) at 5 kg for 15 s. Flexural strength was measured in a four point bending on an Instron universal testing machine (series 8511, Instron Co., Canton, MA, USA). The outer and inner spans were 40 and 20 mm length, respectively. The nominal dimensions of the testing bars were about $3\times4\times45$ mm^3 with 45° edge chamfers. Compressive strength was measured by using the same equipment and calculated according to the 0.2% offset method (yielding stress). The dimensions of the samples are 5 mm in diameter and 10 mm in height.

Fracture toughness was measured in the same testing fixture using a chevron-notched specimen[10,16–20] ($3\times4.5\times30$ mm^3) in three-point bending test with a span of 12 mm and a cross head speed of 0.02 mm/min. The maximum load of the bend test was used to calculate the toughness of the composite according to the following equation;[20]

$$K_{ic} = \frac{P_{max}}{B\sqrt{W}} Y_c(\alpha_0) \quad (1)$$

with:

$Y_c(\alpha_0) = 5.369 + 27.44\alpha_0 + 18.93\alpha_0^2 - 43.42\alpha_0^3 + 338.9\alpha_0^4$,

where P_{max} is the maximum test load, B and W the width and height of the bending bar, respectively, $\alpha_0 = a_0/W$, the dimensionless chevron notch factor, and a_0 the length of chevron tip. For the stable crack growth mode in the chevron-notch three-point bend specimen,[19–21] it is suggested that $W/B = 15$, $\alpha_0 = 0.33$ and the chevron angle $\theta^\circ = 60$.

2.4. Microstructural analysis

The phases of the as-received AlN powders and AlN/Al composites were analyzed by an X-ray diffractometer (Rigaku D/Max-II BX) using Cu K_α radiation (30 KV, 20 mA) in the range of 20–80° at a speed of 4°/min. The polished specimens of the composite were observed and characterized using optical microscope (OP) and image analyzer (Optimas, Vol.1.0, imaging Fundamentals, Tacoma, WA). Each image is divided into nine discrete elements (pixels), and entered into a digital computer to calculate the volume fraction of AlN in the AlN/Al composite. Fracture surfaces and crack propagation behavior were scrutinized using OP and scanning electron microscopy (SEM, Hitachi S-4200).

3. Results and discussion

3.1. Compositional and microstructural analysis

The AlN preforms were made at four selected pressing pressures (10, 30, 40, 60 MPa) and sintered at 1600°C for 1 h in N_2 atmosphere. The porosity is in the range 52.0–31.1 v/o. As the pressing pressure increased, the particle was packed more closely and the preform density was increased, (the porosity decreased). Possible densification stages were previously summarized by MacLeod.[22] Four different sequential processes included: (1) particle rearrangement leading to closer packing; (2) formation of arches and vaults protecting voids and capable of supporting the applied pressure; (3) a combination of elastic, plastic and fracture deformation mechanisms occurring simultaneously and resulting in higher density; and (4) bulk compression of the material itself.

The sintering properties of AlN are mostly determined by its particle size, particle size distribution, the uniformity of particle packing, sintering aids (such as CaO, Y_2O_3, etc.) and sintering condition (temperature, time and atmosphere).[23–25] In this work, carbon was added to prevent sintering and retain open porosity. Almost no densification was observed in AlN even after it was sintered at 1930°C for 16 h with the addition of 1 wt.% carbon.[26]

The AlN/Al composites made from AlN preforms pressed at four different pressures (10, 30, 40, 60 MPa) were designated as A10, A30, A40 and A60, respectively. A typical microstructure of the AlN/Al composite (A30) is shown in Fig. 2(a). Etching is not necessary for such optical microstructural analyses due to the adequate contrast between the bright Al and the gray AlN phases in the composite. Fig. 2(b) indicate that the Al regime is free of defect, however, some very small pores may be isolated or existed in the AlN regime which makes the full infiltration of Al impossible.

3.2. Density measurement

The AlN/Al composites fabricated in this study contain about 1.4 to 23 vol.% porosity, and the densities were in the range between 2.89 and 2.97 g/cm^3. The density is less than fully dense AlN ceramic (3.26 g/cm^3) because the composites contain aluminum of density 2.71 g/cm^3 in addition to the residual pores.

3.3. Mechanical properties

Fig. 3 is the Vickers hardness versus AlN contents of the AlN/Al composites. The hardness increased with the increase of AlN contents. Indentation crack was absent even under the load of 20 kg_w (Fig. 4). Therefore, the fracture toughness of the composite was measured by

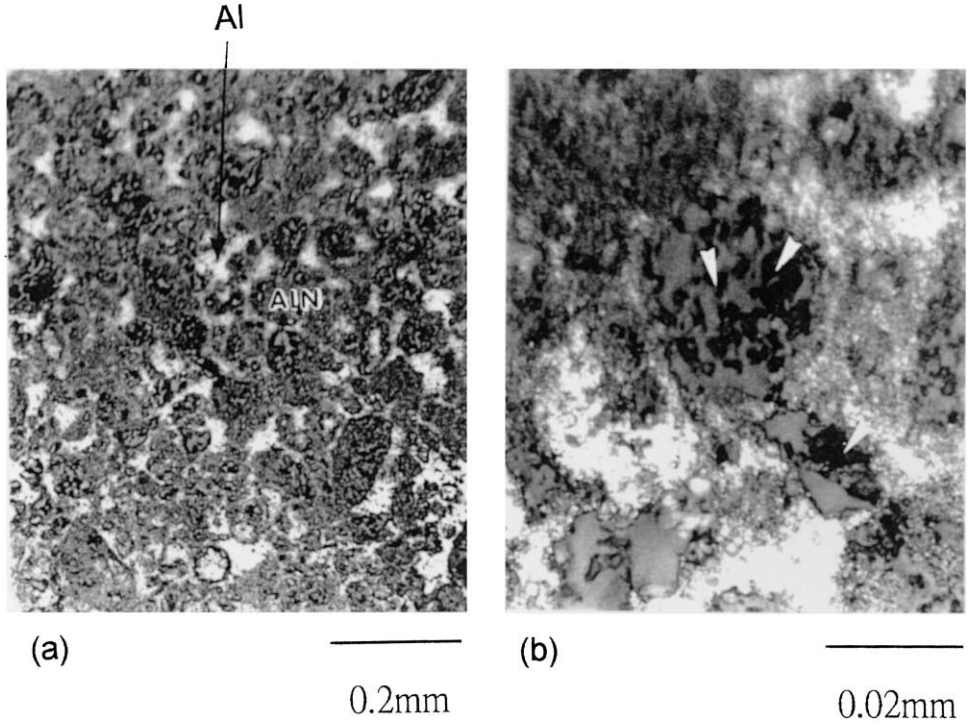

Fig. 2. Optical photographs showing the microstructure of AlN/Al composite (A30). (a) The bright zone are Al and the dark zone are AlN, (b) arrows indicate pores in AlN.

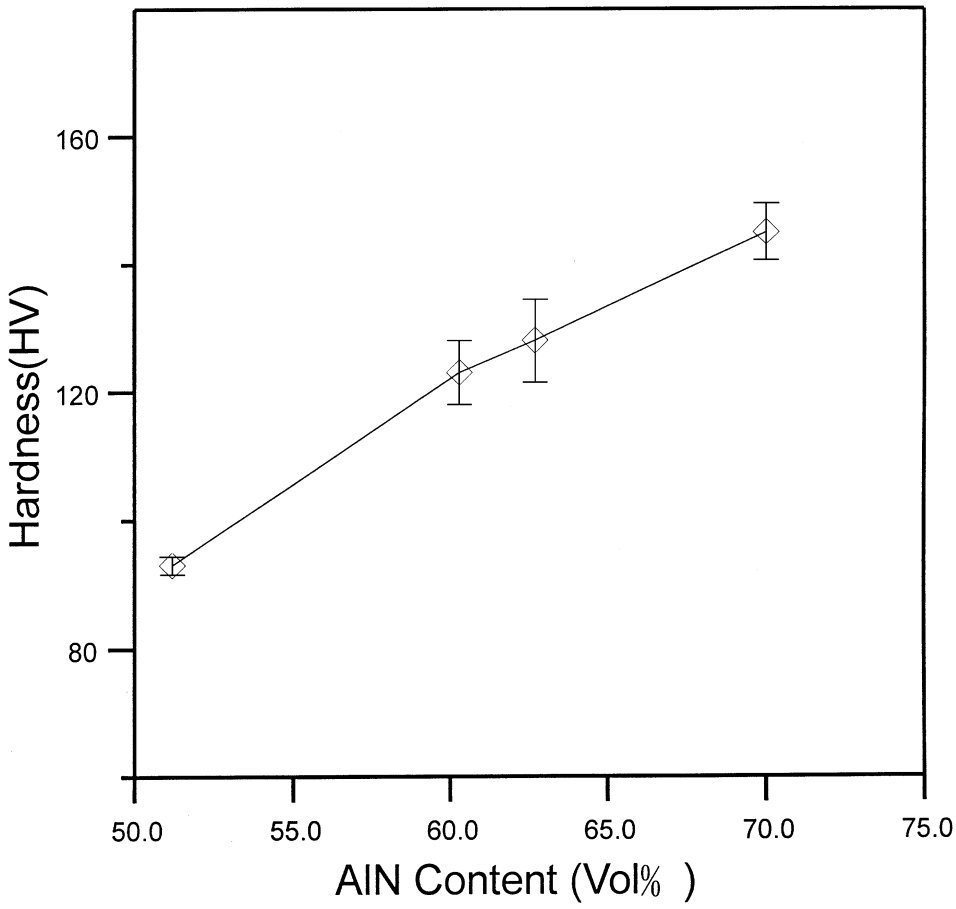

Fig. 3. Vicker's hardness versus AlN contents in the AlN/Al composites.

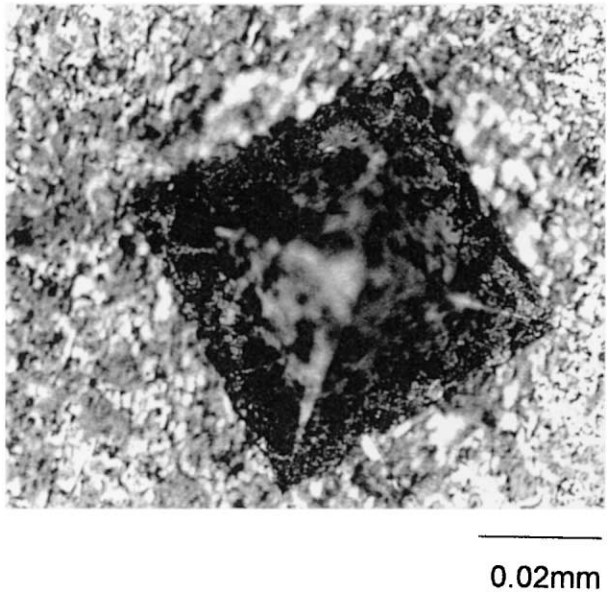

Fig. 4. Optical photograph showing the Vicker's indentation on the polished surface of AlN/Al composites (A30).

three point bending test on chevron-notch specimen[9,10] instead of the indentation method.

3.3.1. Bending strength, fracture surface analysis and compressive strength

Fig. 5 shows the four-point bending strength of AlN/Al composites versus AlN volume content. The bending strengths (328–490 MPa) of the composite are in the same range with dense sintered AlN (280–350 MPa)[27] and basically dependent on the content of AlN. Some specimens sometimes present values higher than 500 MPa, which is comparable with the values reported previously[6] on three-point bending strength of the AlN/Al composites produced by pressureless liquid metal infiltration.

Typical fractographs of fractured surfaces by SEM are presented in Fig. 6. Typically, the aluminum phase has failed by ductile rupture and it is pulled up into ridges on the grain surfaces and some resulted in dimple fracture of ligaments. Meanwhile, the AlN was fractured either by intergranular decohesion for smaller particles or transgranular clevage for large particles. The arrows A and B in Fig. 6(a) indicate ductile dimple rupture of Al and brittle intergranular fracture along smaller AlN grains, respectively. The brittle transgranular fracture of larger AlN grain is marked as C in Fig. 6(b). Therefore, similar to other ceramic-metal composites (such as Al_2O_3/Al[7] and WC/Co [28]), the

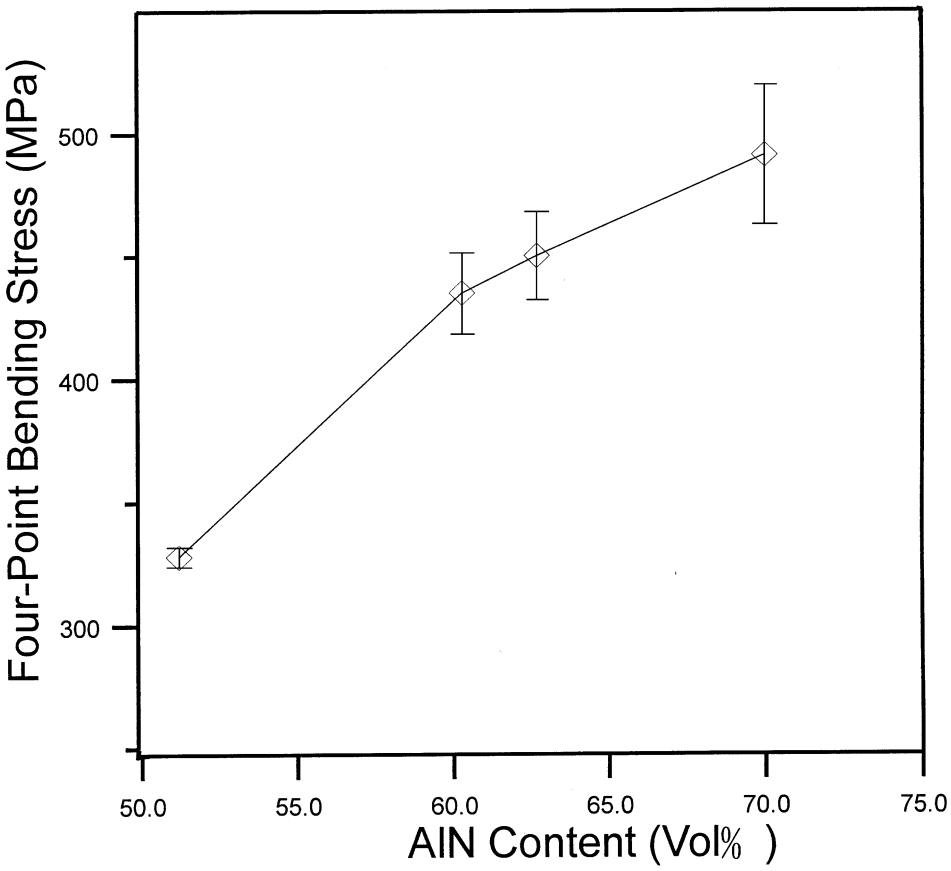

Fig. 5. Bending strength versus AlN volume content of the AlN/Al composites.

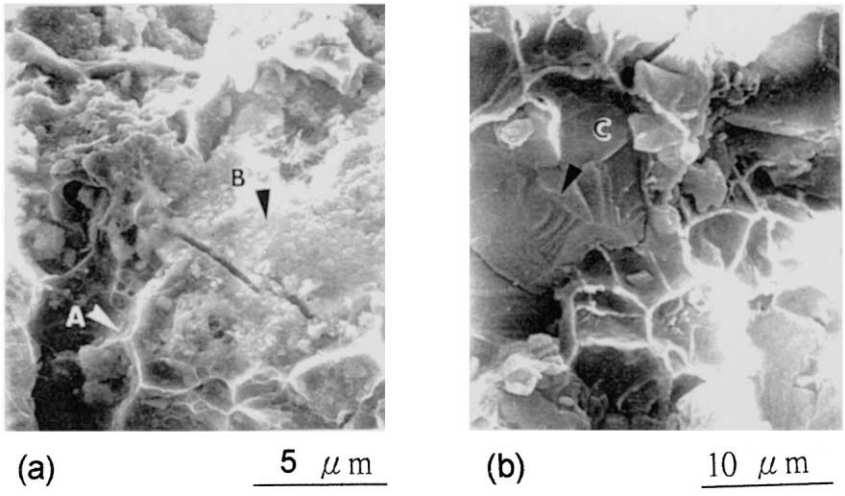

Fig. 6. SEM fractographs of AlN/Al composites (A30) after bending test. (a) Arrows A and B indicate ductile rupture of Al and brittle intergranular fracture of AlN, respectively, (b) arrow C indicates brittle transgranular fracture of AlN.

fracture mechanisms in AlN/Al composite included the ductile fracture in Al, and the intergranular and transgranular brittle fractures along smaller and larger mean grain size of AlN, respectively.

The compressive strength of the AlN/Al composites was between 210 and 340 MPa, and increased with the AlN content.

3.3.2. Fracture toughness and toughening mechanism

Fig. 7 shows the load-displacement curves of the three-point bending test for chevron-notched AlN/Al composite specimen. No catastrophic fracture mode has been observed. Essentially, the curves exhibit quasi-stable crack growth mode even though some noise from the testing fixture has been presented in the curves.

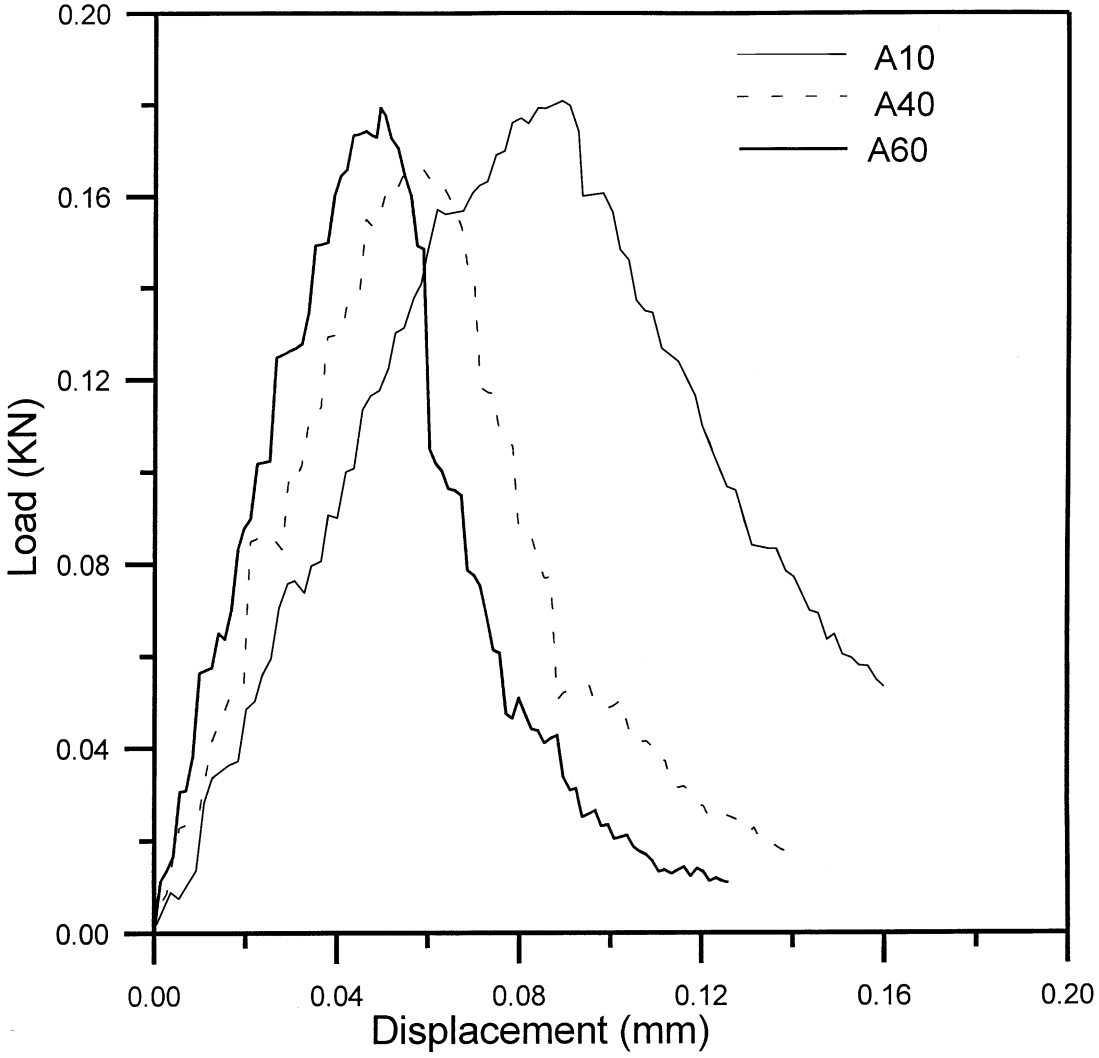

Fig. 7. Load–displacement curves of chevron-notched AlN/Al composites.

Therefore, the maximum load (P_{max}) could be used to calculate the fracture toughness [20,21] of the composite according to Eq. (1) (in Section 2.3).

In addition, Fig. 7 also shows that the ductility of the composite decreased with the increase of AlN content due to the reduction of ductile metal content.

Fig. 8 shows the fracture toughness of the AlN/Al composites versus AlN volume content. The fracture toughness of the squeeze casting AlN/Al composites was between 14.5 and 15.7 MPa $m^{1/2}$ and was independent on the change of the composition. This value is about four times of that hot-pressed AlN ceramic (with mean grain size of 10 μm, 3.6 MPa $m^{1/2}$).[29] Similar high degrees of toughening has been observed in (1) WC (with mean grain size of 2.2 μm) reinforced with Co network (~20 MPa $m^{1/2}$) [30]; and (2) toughness of $MoSiO_2$ (with mean grain size of 200 μm) which was increased from 3.3 to about 15 MPa $m^{1/2}$ with the incorporation of Nb fibres (with diameter of 250 μm) or foils (with thickness of 250 μm).[10]

To observe possible bridging zone effects, a chevron notch three-point bend test was interrupted after maximum load. The specimen was carefully moved away from the test fixture and vacuum-imbeded with epoxy to prevent crack propagation during the subsequent grinding and polishing procedures. Fig. 9 shows the optical photographs of the crack growth path in AlN/Al composite (A30). It indicates that the crack advances in several ways: rupture of Al phases (arrow A), intergranular debonding along AlN/AlN (arrow B) and AlN/Al boundary (arrow C), or transgranular fracture along AlN grains.

Some spectacular bridging ligaments of Al have also been observed between the crack faces as shown in Fig. 10. The black arrow indicates the ligament zone. The white arrow indicates a broken ligament zone. The surface fracture paths appear to be interrupted by the Al ligaments, as if the primary crack stopped by those ligaments and then reinitiated on the other side or, more likely moved around in the third dimension.

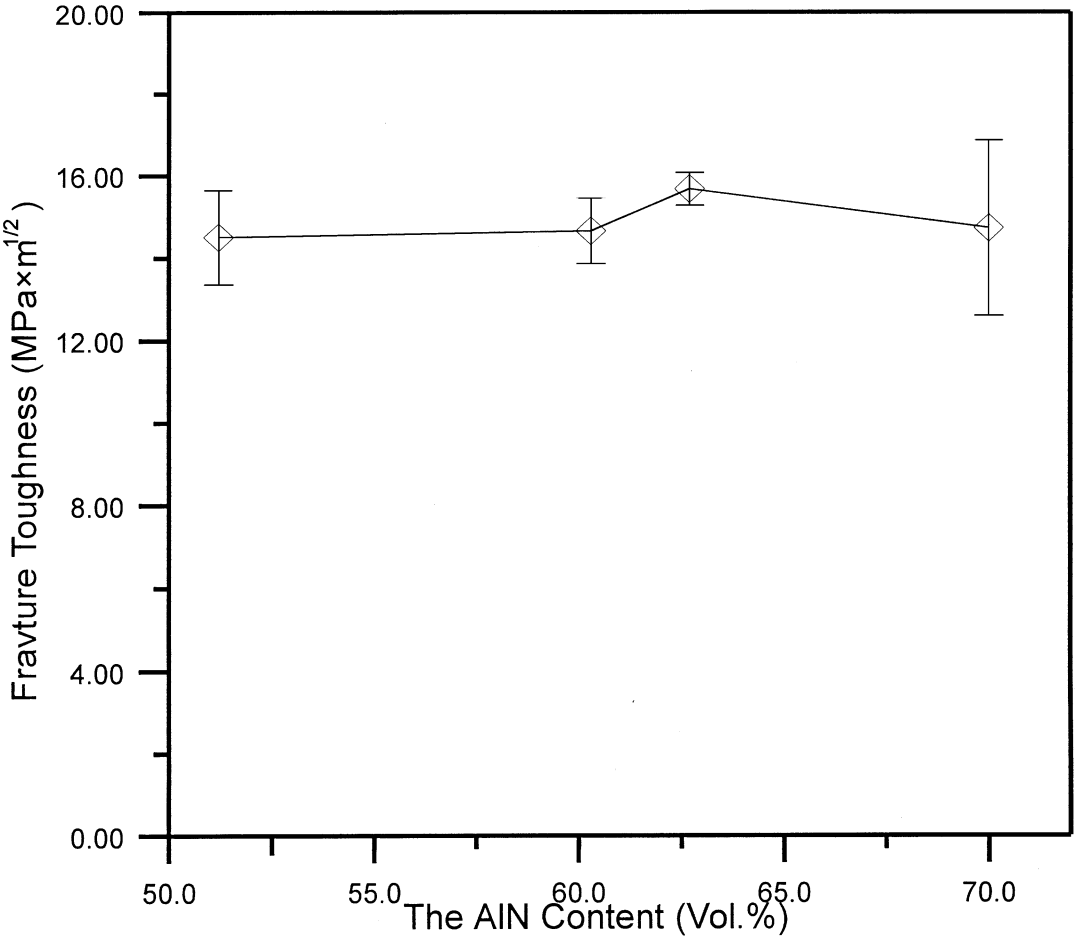

Fig. 8. The fracture toughness of the AlN/Al composites versus AlN volume content.

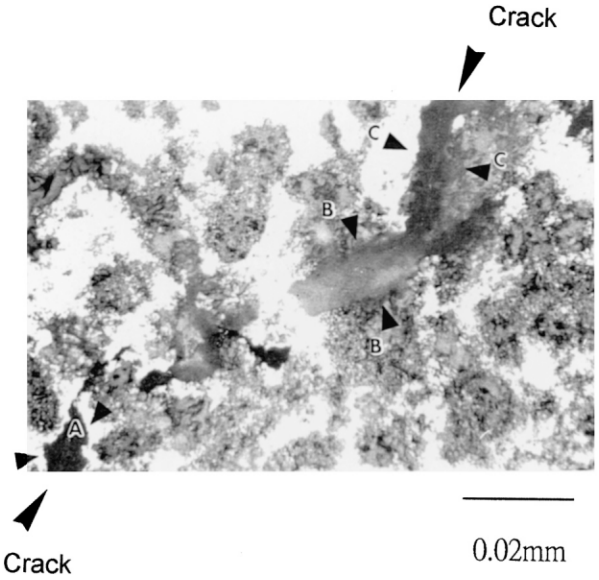

Fig. 9. Optical photograph showing the crack growth path in AlN/Al composite (A30). The crack growth paths include along Al/Al interface (arrow A), AlN/AlN interface (arrow B) and AlN/Al interface (arrow C).

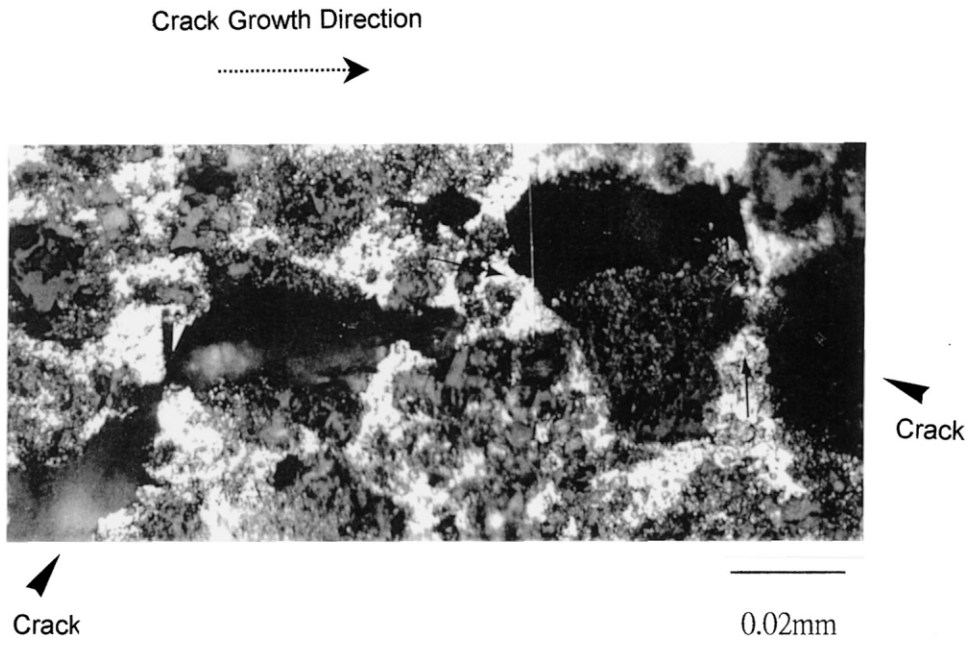

Fig. 10. Optical photograph showing the crack growth path in AlN/Al composite (A30). The black arrow indicates the ligament zone. The white arrow indicates one broken ligament zone. The direction of dotted line means crack growth path.

4. Summary and conclusion

1. As the pressing pressures of AlN preforms increased from 10 to 60 MPa, the AlN content in AlN/Al composite increased from 51.2 to 70.0%. The hardness of the composite increased from 93 to 145 Hv, the fracture strength increased from 328 to 490 MPa, and the compressive strength increased from 210 to 340 MPa for the corresponding composites.
2. The fracture modes in AlN/Al composites included (1) ductile neck fracture in Al, (2) brittle intergranular fracture between smaller AlN grains, and (3) brittle transgranular fracture within larger AlN grain.
3. The crack growth paths in AlN/Al composites included (1) Al/Al interface, (2) AlN/AlN interface, and (3) AlN/Al interface.
4. The fracture toughness of squeeze casting AlN/Al composites was between 145 and 15.7 MPa $m^{1/2}$, which is independent on Al content. However, the ductility of the composite decreased with the increase of AlN.

References

1. Long, G. and Foster, L. M., Aluminum nitride, a refractory for aluminum to 2000°C. *J. Am. Ceram. Soc.,* 1959, **42**(2), 53–59.
2. Toy, C. and Scott, W. D., Wetting and spreading of molten aluminum against AlN surfaces. *J. Mater. Sci.,* 1997, **32**, 3243–3248.
3. Iwase, N., Tsuge, A. and Sugirua, Y., Development of a high thermal conductive AlN ceramic substrate technology. *Int. J. Hybrid Microelectronics,* 1984, **7**(4), 49–53.
4. Werdecker, W. and Aldinger, F., Aluminum nitride, an alternative ceramic substrate for high power applications in microcircuits. *IEEE Trans. on Components, Hybrids and Mgf. Tech.,* 1983, **7**(4), 399–404.
5. Savrun, E., Tan, C. Y. and Robinson, J. In *Proceedings of the 22nd SAMPE Technical Conference, Boston, MA*, ed. D. Michelooe *et al*. The Society for the Advancement of Material and Process Engineering, Covina, CA, 1990, pp. 619.
6. Toy, C. and Scott, W. D., Ceramic-metal composite produced by melt infiltration. *J. Am. Ceram. Soc.,* 1990, **73**(1), 97–101.
7. Flinn, B. D., Rühle, M. and Evans, A. G., Toughening in composites of reinforced with Al. *Acta Metall.,* 1989, **37**(11), 3001–3006.
8. Halverson, D. C., Pyzik, A. J., Aksay, I. A. and Snowden, W. E., Processing of boron carbide/aluminum composites. *J. Am. Ceram. Soc.,* 1988, **72**(5), 775–780.
9. Sigl, L. S. and Fischmeister, H. F., On the fracture toughness of cemented carbides. *Acta Metall.,* 1988, **36**(4), 887–897.
10. Shaw, L. and Abbaschian, R., Toughening $MoSi_2$ with niobium metal-effects of morphology of ductile reinforcement. *J. Mater. Sci.,* 1995, **30**, 849–854.
11. Creber, D. K., Poste, S. D., Aghajanian, M. K. and Claar, T. D., AlN composite growth by nitridation of aluminum alloys. *Ceram. Sci. Proc.,* 1988, **7–8**, 975–982.
12. Inoue, A., Nosaki, K., Kim, B. G., Yamaguchi, T. and Masumoto, T., Mechanical strength of ultra-fine Al–AlN composites produced by a combined method of plasma-alloy reaction, spray deposition and hot pressing. *J. Mater. Sci.,* 1993, **28**, 4398–4404.
13. Lai, S. W. and Chung, D. D. L., Fabrication of particulate aluminium-matrix composites by liquid metal infiltration. *J. Mater. Sci.,* 1994, **29**, 3128–3150.
14. Ray Siba, P. and Yun David, I., Squeeze-cast ceramic-metal composites. *Ceram. Bull.,* 1991, **70**(2).
15. Yue, T. M. and Chadwick, G. A., Squeeze casting of light alloys and their composites. *J. Mater. Proc. Technol.,* 1996, **58**, 302–307.
16. Barker, L. M., A simplified method for measuring plane strain fracture toughness. *Eng. Fract. Mech.,* 1977, **9**, 361–369.
17. Munz, D., Bubsey, R. T. and Srawley, J. E., Compliance and

stress intensity coefficients for short bar specimens with chevron notches. *Int. J. Fract.,* 1980, **16**(4), 359–374.
18. Munz, D., Bubsey, R. T. and Shannon, J. L., Jr., Fracture toughness determination of Al_2O_3 using four-point-bend specimens with straight-through and chevron notches. *J. Am. Ceram. Soc.,* 1980, **6**, 300–305.
19. Shih, T. T., An evaluation of the chevron V-notched bend bar fracture toughness specimen. *Eng. Fract. Mech.,* 1981, **14**(4), 821–832.
20. Wu, S.-X., Fracture toughness determination of bearing steel using chevron-notch three point bend specimen. *Eng. Fract. Mech.,* 1984, **19**(2), 221–232.
21. Shang-Xian, Wu., Stability and optimum geometry of chevron notched three point bend specimens. *Int. J. Fract.,* 1984, **26**, R43–R47.
22. MacLeod, H. M., Compaction of ceramics. In *Enlargement and Compaction of Particulate Solids*, Chapter 11, *Butterworths Monographs in Chemical Engineering*, ed. Nayland G. Stanley-Wood. Butterworth & Co., London, 1983 (Chapter 11) pp. 253–261.
23. Troczynski, T. B. and Nicholson, P. S., Effect of additives on the pressureless sintering of aluminum nitride between 1500°C and 1800°C. *J. Am. Ceram. Soc.,* 1989, **72**(8), 1488–1491.
24. Kurokawa, Y., Utsumi, K. and Takamizawa, H., Development and microstructual characterization of high-thermal conductivity aluminum nitride ceramics. *J. Am. Ceram. Soc.,* 1988, **71**(7), 588–594.
25. Richerson, D.W., Theory of sintering, section 7.1 In *Modern Ceramic Engineering, Properties, Processing, and Use in Design, Manufacturing Engineering and Material Science Processing/8*, Marcel Dekker, Inc., New York, 1982.
26. Horvath, S. F., Witek, S. R. and Harmer, M. P., Effects of carbon and calcium oxide on the sintering behavior of aluminum nitride. In *Ceramic Substrates and Packages for Electronic Applications*, ed. M. F. Yan and K. Niwa *et al.* Advances in Ceramics, Vol. 26. Arerican Ceramic Society, Westerville, Ohio, 1989, pp. 121–131.
27. Suryanarayana, D., Oxidation kinetics of aluminum nitride ceramics. *J. Am. Ceram. Soc.,* 1990, **73**(4), 1108–1110.
28. Slesar, M., Dusza, J. and Parilak, L., Micromechanics of fracture in WC/Co hard metals. *Inst. Phys. Conf. Ser.,* 1986, **75**, 657.
29. Witek, S. R., Miller, G. A. and Harmer, M. P., Effects of CaO on the strength of AlN. *J. Am. Ceram. Soc.,* 1989, **72**(3), 469–473.
30. Chermant, J. L. and Osterstock, F., Fracture toughness and fracture of WC–Co composites. *J. Mater. Sci.,* 1976, **11**, 1939–1951.